Chapter 2

Review of optical, optomechanical systems and nonclassical effects

2.1 Introduction

COM, a branch of quantum optics, is too much interesting and has fundamental insight. It has also been attracting the researcher in last few decades both in theoretical illustration and experimental works. It lies in the intermediary between quantum and classical mechanics and also provides the practical ground to note quantum jumps of a mechanical system. In an optomechanical system (OMS) electromechanical degrees of freedom and macroscopic or mesoscopic mechanical objects are coupled via radiation pressure interaction.

In 1970, A. Ashkin first demonstrated that motion of the dielectric balls can be speeded up and trapped via radiation-pressure force [41]. Followed by this result, a lot of works have been performed such as realization of optical tweezers, gravitational wave detectors [42, 43]. Light-matter interaction is mainly two types – non-resonant and resonant. Generally, non-resonant interactions are wavelength independent, so this provides the ground for optomechanical interactions for a wide regime – microwave to optical range. On the other hand, resonant interaction gives the possibility of enhanced interaction but it is restricted by narrow span of wavelengths. COM exploits the finest by fulfilling resonant enhancement via resonant structure rather than the internal structure of the used material. This would be an example, optical resonator with a sequence of narrow resonances. Indeed, a lot of designs can acquire optomechanical control in high-Q resonators via radiation pressure interaction. The designs range from centimetre size macroscopic mirror to nano-meter structures (10^7 atoms).

Braginsky and Manukin, first experimentally established optomechanical effects at microwave domain in 1967 [44]. A. Dorsel et al established radiation-pressure induced

effect at optical regime in 1983 [45]. In connection to these, the heating or cooling effect of the mechanical motion is possible. This is due to finite delay in time between the response of optical field and mechanical motion (details of the cooling effect is discussed in next section 2.4). In that context, the researchers realized basic quantum optical effects on mechanical detection (such as standard quantum limit) and how the interaction can create nonclassical states in optical field.

2.2 Optical and Optomechanical systems

Optical microcavity, optical microresonator, microdisks, microring, microtoroids all are interesting and promising candidates to study different nonlinear and nonclassical effects. For example, optical WGM micro-toroidal resonators can confine and trap light in small volume of space by means of total internal reflection around the perimeter of the dielectric-air confluence. These characteristics enrich nonlinear interaction and also intensity of light.

During 1990s, cavity OMSs were started to analyze theoretically via quantum nondemolition (QND) estimation, squeezing of light etc. Followed by these, a lot of theoretical investigation and experimental work have been done in different OMSs [46-51]. In different experimental technique, a large variety of optomechanical set up have been demonstrated, such as suspended macroscopic mirrors/ micro-pillars/ micro-mirrors in a cavity, mechanical membrane placed inside a cavity, hybrid OMSs, semiconductor micro-disk resonator, double-disk micro-resonator, near-field coupled nano-mechanical oscillator, optical microsphere resonator, membrane in a superconducting microwave circuit, photonic crystals patterned into nano-beams, cold atoms in a cavity etc [52, 53]. In this work, we have studied OMS, cavity inside

membrane in chapter 3 and two-cavity system in chapter 4. In chapter 5, we have studied optical system with two micro-cavities. Figure 2.1 shows typical micro-cavity and OMS set up.

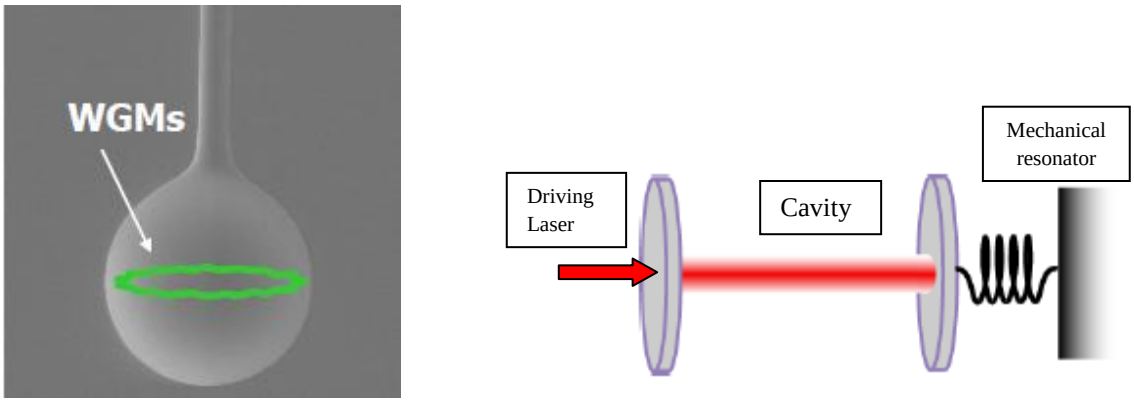

(a) (b)

Figure 2.1: Schematic representation of (a) WGM micro-cavity (b) OMS set up with external driving.

2.3 Optical and Mechanical resonators

From the previous discussion, it is clear different types of optical and optomechanical configurations are possible. Here, we have resumed the basic properties of optical cavities and mechanical resonators.

2.3.1 Optical resonator

We consider a Fabry-Perot etalon or resonator which consists of two high reflective mirrors. The angular frequency for m th mode is given by $\omega_{c,m} = m\,\pi c/L$, where L is the separation between two mirrors. For single mode the frequency is denoted by ω_c. The FSR (free spectral range) or the difference between two longitudinal successive resonance frequencies is given by $\delta\omega_{FSR} = \pi c/L$. The optical finesse measures the mean of round-trips of a photon before leaving the cavity $\mathcal{F} \equiv \delta\omega_{FSR}/\kappa$. The quality factor is $Q = \omega_c/\kappa$, where κ denotes the total decay rate of the cavity. Generally, total

loss rate has two distinct parts: $\kappa = \kappa_i + \kappa_{ex}$, κ_i refers intrinsic loss rate and κ_{ex} is the decay rate associated with external coupling [53].

If the cavity field is characterized by operator $\hat{a}$, then according to input-output formalism, the expression of the output field from the resonator is given by

$$\hat{a}_{out} = \hat{a}_{in} - \sqrt{\kappa_{ex}}\hat{a} \tag{2.1}$$

The steady state cavity photon number is given by

$$\hat{n}_c = |\langle\hat{a}\rangle|^2 = \frac{4\kappa_{ex}}{4\Delta^2+\kappa^2}|\langle\hat{a}_{in}\rangle|^2 = \frac{4\kappa_{ex}}{4\Delta^2+\kappa^2}\frac{P}{\hbar\omega_L} \tag{2.2}$$

where P denotes the input power of the laser with frequency ω_L and Δ indicates frequency detuning between the cavity and the laser field.

The reflection amplitude from the cavity is given by

$$\Re = \frac{\langle\hat{a}_{out}\rangle}{\langle\hat{a}_{in}\rangle} = \frac{(\kappa_i-\kappa_{ex})-2i\Delta}{(\kappa_i+\kappa_{ex})-2i\Delta} \tag{2.3}$$

From the above equation (2.3), the probability of reflection $|\Re|^2$ can be calculated. The expression of $|\Re|^2$ can define three distinct regimes. First, under coupling $(\kappa_i \gg \kappa_{ex})$ - the intrinsic decay rate is larger. This condition is not suitable as it provides an effective loss. Second, critical coupling $(\kappa_i = \kappa_{ex})$ - at resonance $(\Delta = 0)$ this condition leads to $\Re = 0$. This indicates that input power is either totally transmitted through 2nd mirror or dissipated in the cavity. Third, over coupling $(\kappa_i \ll \kappa_{ex})$ - the external coupling is larger. For this case $|\Re|^2 \approx 1$, which imply that without any absorption pump photons emerge from the resonator (quantum limited detection).

2.3.2 Mechanical resonator

The vibrational modes of a system can be obtained by solving the EOM under suitable boundary conditions.

The EOM of a harmonic oscillator with the global amplitude $x(t)$ and effective mass m_{eff} is given by [54, 55]

$$m_{eff}\left[\frac{d^2x(t)}{dt^2}+\gamma\frac{dx(t)}{dt}+\Omega_m^2x(t)\right]=F_{ext}(t) \tag{2.4}$$

where $F_{ext}(t)$ indicates sum of all forces (external force, thermal Langevin force etc) acting on the oscillator. The frequency of mechanical vibration is Ω_m and mechanical damping rate is γ. These are related to mechanical Q factor through the relation $Q_m = \Omega_m/\gamma$.

The quantum mechanical analysis of the mechanical oscillator forms the Hamiltonian as follows:

$$\hat{H}=\hbar\Omega_m\left(\hat{b}^\dagger\hat{b}+\frac{1}{2}\right) \tag{2.5}$$

Here, $b^\dagger(b)$ denote creation (annihilation) of phonon field mode and related with position and momentum operators as

$$\hat{x}=x_{ZPF}\left(\hat{b}^\dagger+\hat{b}\right),\ \hat{p}=im_{eff}\Omega_m x_{ZPF}\left(\hat{b}^\dagger-\hat{b}\right) \tag{2.6}$$

Where $x_{ZPF}=\sqrt{\hbar/2m_{eff}\Omega_m}$ is zero-point fluctuation amplitude of the oscillator.

The spreading of the field co-ordinate in ground state $x_{ZPF}^2=\langle 0|\hat{x}^2|0\rangle$, here $|0\rangle$ implies vacuum state of the mechanical mode. The average value of the phonon number is given by $\bar{n}=\langle b^\dagger b\rangle$.

To illustrate the effect of dissipation, we consider the oscillator is linked to a high temperature bath. The phonon number governed by the following equation

$$\frac{d\bar{n}}{dt}+\gamma(\bar{n}-\bar{n}_{th})=0 \tag{2.7}$$

The initial state of the oscillator is the ground state i.e. at $t=0,\ \bar{n}=0$. The time dependence of the mean phonon number is given by $\bar{n}(t)=\bar{n}_{th}(1-e^{-\gamma t})$. Using this expression, the mean thermal phonon number can be obtained as $\bar{n}_{th}=k_BT/\hbar\,\Omega_m$,

which measures the thermal decoherence. High Q cavity and low-temperature bath is required to achieve low decoherence. For Fock state $|n\rangle$ basis, the change of the population is expressed by quantum master equation. The decoherence rate [56] is given by $(n+1)\bar{n}_{th}\gamma + n(\bar{n}_{th}+1)\gamma$, which implies that higher Fock state shows higher rate of decoherence.

2.4 Basic cavity optomechanics

We have discussed basic COM via optomechanical coupling and radiation pressure interaction between mechanical and optical mode. The mechanism of cavity cooling also has been discussed.

2.4.1 Radiation pressure & optomechanical coupling

Here, we describe radiation pressure which couples the optical field with the mechanical oscillator. It arises due to transfer of momentum of the optical field to the oscillator and which corresponds to the Poynting vector. In a Febry-Perot resonator the momentum transfer by single photon is $2h/\lambda$ (λ is wavelength of photon). The corresponding force due to radiation-pressure is

$$F = \frac{\hbar\omega_c}{L}\langle\hat{a}^\dagger\hat{a}\rangle = \hbar G\langle\hat{a}^\dagger\hat{a}\rangle = \hbar G|\alpha|^2 \tag{2.8}$$

Force due to one cavity photon is $\hbar\omega_c/L$. The frequency pull factor $G = \omega_c/L$, denotes the change of frequency with position. The mean value of the photon number is $\alpha = \sqrt{\langle\hat{a}^\dagger\hat{a}\rangle}$.

Generally, optomechanical coupling arises due to following cases: direct momentum transfer (Febry-Perot cavity with movable mirror, micro-toroids), optical near field effects (nano systems in the evanescent field of a cavity), dispersive cavity frequency shift (membrane inside a resonator) [52, 53, 57, 58].

For an uncoupled system the Hamiltonian reads as

$$\hat{H}_{sys} = \hbar\omega_c \hat{a}^\dagger \hat{a} + \hbar\Omega_m \hat{b}^\dagger \hat{b} \tag{2.9}$$

The resonance frequency is modified via mechanical displacement as

$$\omega_c(x) = \omega_c + x\frac{\partial\omega_c}{\partial x} + \cdots \tag{2.10}$$

For simplicity, we restrict up-to linear term and re-define frequency change per displacement as $G = -\frac{\partial\omega_c}{\partial x}$. After modulation, the Hamiltonian of cavity part becomes $\hbar\omega_c(x)\hat{a}^\dagger\hat{a} \approx \hbar(\omega_c - G\hat{x})\hat{a}^\dagger\hat{a}$. So, the interaction part of Hamiltonian is

$$\hat{H}_{int} = -\hbar G\hat{x}\hat{a}^\dagger\hat{a} = -\hbar g_0 \hat{a}^\dagger\hat{a}\,(\hat{b}^\dagger + \hat{b}) \tag{2.11}$$

Here, the optomechanical vacuum coupling strength (in terms of frequency) is $g_0 = Gx_{ZPF}$ .This quantifies interaction between a single phonon and a photon.

The force due to radiation-pressure can also be written as (function of g_0)

$$F = -\langle\frac{d\hat{H}_{int}}{d\hat{x}}\rangle = \frac{\hbar g_0}{x_{ZPF}}\langle\hat{a}^\dagger\hat{a}\rangle$$

If the interaction part is linearized by means of $\hat{a} = \bar{\alpha} + \delta\hat{a}$ i.e. the optical field is expressed as sum of coherent amplitude $\bar{\alpha}$ and small fluctuation part $\delta\hat{a}$. The equation (2.11) takes the form

$$\hat{H}_{int}{}^{lin} = -\hbar g_0\bar{\alpha}(\delta\hat{a}^\dagger + \delta\hat{a})\big(\hat{b}^\dagger + \hat{b}\big) = -\hbar g(\delta\hat{a}^\dagger + \delta\hat{a})\big(\hat{b}^\dagger + \hat{b}\big) \tag{2.12}$$

Here, $g = g_0\bar{\alpha}$ termed as effective coupling strength. Another interesting condition $g > k$, termed as strong-coupling regime. Experimentally it is challenging to reach the regime. At this regime, different quantum nonlinear effects become observable.

Depending on cavity detuning, three distinct regimes are possible w.r.t. the interaction. First, Resonance condition ($\Delta = 0$): at this interaction part is same as in equation (2.12).

It is clear that $\hat{x} \propto \left(\hat{b}^{\dagger} + \hat{b}\right)$, which provides an amount of phase shift of the optical field and this condition turns up in detection of optomechanical displacement. This Hamiltonian also is viewed as achieving quantum non-demolition (QND) detection [59-61] of the light field amplitude quadrature $(\delta\hat{a}^{\dagger} + \delta\hat{a})$. Second, blue-detuned regime ($\Delta \approx +\Omega_m$): employing RWA it is obtained that non-resonant terms are dominant. So, interaction Hamiltonian takes the form $-\hbar g\left(\delta\hat{a}^{\dagger}\hat{b}^{\dagger} + \delta\hat{a}\,\hat{b}\right)$. If the dissipation is absent, the energies are conserved in both the mode. There is an exponential growth of energy, which is interpreted as amplification or anti-damping. This is useful for parametric amplification [62]. If the dissipation is low, this may generate a dynamical instability and that provides self-induced oscillations of the mechanical system. Third, red-detuned regime ($\Delta \approx -\Omega_m$): where two oscillators (cavity field and mechanical field) having same frequency (nearly) and interchange quanta. So, non resonant terms $\left(\delta\hat{a}^{\dagger}\hat{b}^{\dagger}, \delta\hat{a}\,\hat{b}\right)$ should be omitted and interaction part becomes $-\hbar g\left(\delta\hat{a}^{\dagger}\hat{b} + \delta\hat{a}\hat{b}^{\dagger}\right)$ which refers as beam-splitter interaction. This condition is related to opto-mechanical cooling (thermal phonons transfer to cold photon mode) [63].

2.4.2 Cavity Cooling

Due to interaction of radiation pressure the cavity length changes, which lead to change in optical field phase and intensity. This provides two main effects. First, optical spring effect – optically influenced change in the frequency of the mirror oscillation that can provide a considerable reinforcing of its effective frequency. From the expression of mean phonon number $\bar{n}_{th} = k_B T/\hbar\,\Omega_m$, it is evident that for constant temperature, $\bar{n}_{th}$ reduces as Ω_m increases. So, the system can attain quantum regime (reduction of the

temperature is not required). Second, cold damping or optical damping – the optical field seems like a viscous fluid that resist the motion of the mirror and it leads to cooling of center-of-mass motion. In absence of the optical field, the mirror is coupled to the temperature bath, dissipatively. When optical field is present, an extra damping channel is required to consider. So, the energy (center-of-mass) equation becomes [52, 53]

$$\frac{d}{dt}\langle E\rangle = -\gamma\langle E\rangle + \gamma k_B T - \Gamma_{om}\langle E\rangle \tag{2.13}$$

Where $\Gamma_{om} = \frac{2\hbar G^2|\alpha|^2}{m_{eff}k\Omega_m}$, is the optomechanical decay rate. As mechanical frequency is lower than optical frequency, so at low temperature $(T \approx 0)$ coupling of the optical field with reservoir, is more effective. In steady state, the expression of energy is given by $\langle E\rangle = \gamma k_B T/(\gamma + \Gamma_{om})$. So, effective temperature is

$$T_{eff} = \frac{\gamma T}{(\gamma+\Gamma_{om})} = \frac{\gamma T}{\gamma_{eff}} \tag{2.14}$$

So, controlling optomechanical coupling and hence Γ_{om}, the effective temperature can be lowered. Alternatively, the line-width widens and area of the displacement spectrum is reduced (figure 2.2 a), which leads to cooling effect.

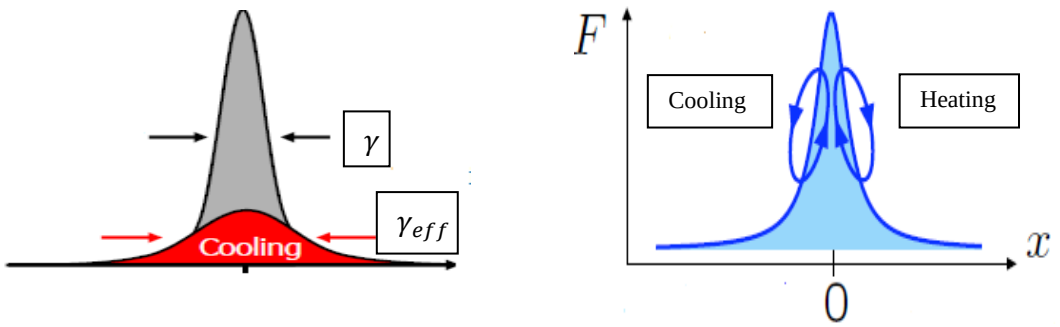

(a) (b)

Figure 2.2: (a) spreading of decay line width (b) work done leads to cooling and heating

The above classical derivation is not exact in some cases and can't anticipate cooling limits [64, 65]. So, quantum mechanical analysis is required for exact cooling. There are several approaches such as quantum noise approach for weak coupling regime, covariance approach both for weak as well as strong coupling regime [66]. In 2006, three research groups reported radiation pressure cooling in different OMS such as micromirrors [67, 68] and microtoroids [69]. Cooling in resolved sideband regime realized in 2008 [70]. At the same time, few experimental demonstrations were done based on dynamical back-action process for cooling (temperature is order of few K or mK) [50, 67, 71]. Recently, ground state cooling of the mechanical motion was realized by several groups both in microwave domain [72, 73] and optical domain [74-76]. In 2013, Liu et al proposed the dynamical process of cooling in strong coupling [77]. Figure 2.2 b indicates the cooling when work is done by mechanical system and for heating, work is done by optical field.

In connection, typical scales of COMs experimental parameters are epitomized in Table 2.1 as follows:

References	Membrane frequency (Hz) $\omega_m/2\pi$	Coupling strength (Hz) $g_0/2\pi$	Mass (m) of mechanical system (gm)	Cavity decay rate(Hz) $k/2\pi$	Mechanical damping (Hz) $\gamma/2\pi$	Quality factor Q
O. Arcizet et al. [68]	8.2×10^{5}	1.2	1.9×10^{-4}	1×10^{6}	81	10^{4}
D. Kleckner et al. [78]	9.7×10^{3}	2.2×10^{1}	1.1×10^{-7}	4.7×10^{5}	1.3×10^{-2}	10^{6}
J. Thompson et al. [71]	1.3×10^{5}	5×10^{1}	4×10^{-8}	5×10^{5}	1.2×10^{-1}	10^{6}
E. Verhagen et al. [76]	7.8×10^{7}	3.4×10^{3}	1.9×10^{-9}	7.1×10^{6}	3.4×10^{3}	10^{4}
J. Chan et al. [74]	3.9×10^{9}	9×10^{5}	3.1×10^{-13}	5×10^{8}	3.9×10^{4}	10^{5}
K. Murch et al. [79]	4.2×10^{4}	6×10^{5}	4×10^{-19}	6.6×10^{5}	1×10^{3}	10^{3}

Table 2.1: Experimental parameters for different COMs setup

2.5 Quasi Probability distribution

An important counterpart is visualization for simulation of quantum states (QS). Visualization indicates how the density matrices or state vectors transform with time. Generally, one can be minded that it is the plot of expectation values of a particular operator. The expectation values are calculated from probability distribution (PD). The PD of Fock basis gives the occupation probability of discrete states. The phase-space PD-like-functions give the full description of QS. These are termed as quasi-PD functions. The PD for these functions is negative. The negativity indicates that the state is nonclassical.

For mixed state the density operator is written as

$$\hat{\rho} = \sum_i p_i \, |\varphi_i\rangle\langle\varphi_i| \tag{2.15}$$

where p_i is the probability of $i-th$ state. In terms of number states, $\hat{\rho}$ is

$$\hat{\rho} = \sum_n \sum_m |m\rangle \, \rho_{mn} \langle n| \tag{2.16}$$

where the matrix element ρ_{mn} is $\langle m|\hat{\rho}|n\rangle$. The diagonal elements ρ_{nn} represent the probabilities of finding of the n photons in a field. Another way to represent $\hat{\rho}$ in terms of coherent states as

$$\hat{\rho} = \int P(\alpha) \, |\alpha\rangle\langle\alpha| d^2\alpha \tag{2.17}$$

where the weight function $P(\alpha)$ is termed as Glauber-Sudarshan P function [39, 80, 81]. The right side of the equation (2.17) represents diagonal form of $\hat{\rho}$ and $P(\alpha)$ is analogous with statistical phase-space distribution. Here, the variables of the phase-space are real and imaginary values of α. As $\hat{\rho}$ is Hermitian, $P(\alpha)$ is real. Also $Tr(\hat{\rho}) = \int P(\alpha) \, d^2\alpha = 1$. The states for which $P(\alpha)$ is no more singular than $\delta-$function or positive are termed as classical. But for the states for which $P(\alpha)$ is highly singular than $\delta-$function or negative are, nonclassical. Other important quasi-PD functions are

Wigner function [15], Husimi Q-function [82] etc. The negativity of Wigner and P-functions give the signature of nonclassicality. The zeros of Husimi Q-function correspond to nonclassical behaviour. In the next section, we define different nonclassical effects and their quantifying criteria. Details of the quasi-PD functions with possible applications can be found in reference [83].

2.6 Nonclassical effects

The theoretical idea of nonclassical state was originated from the evolutions of Gaussian wavepackets by Schrodinger, Kennard and Darwin (1926-27), via prototypes of squeezed states [84]. The first experimental evidence of nonclassical state was demonstrated by R. Slusher group [85], in atomic sodium vapour (1985). Using these ideas, possibility of various types of nonclassical effects is reported in different optical system, both theoretically and experimentally [21, 24, 86-91]. These are quadrature squeezing, phase squeezing, spin squeezing, polarisation squeezing, antibunching, intermodal entanglement, EPR steering, Bell states, negativity of Wigner function and Q-function etc. These are quantified by logarithmic negativity, Fano factor, Mandel Q factor, different inequalities etc. In this work, we have analyzed different nonclassical effects which are described in chapter 3, 4 and 5, respectively.

2.6.1 Squeezing

Squeezing is defined as quantum mechanical fluctuation of quadratures. Any quadrature is less noisy than a vacuum or coherent state. Squeezed states have applications in phase estimation [92], quantum imaging [93], weak force detection [94], GEO600 detector [95] and LIGO detector [96] etc.

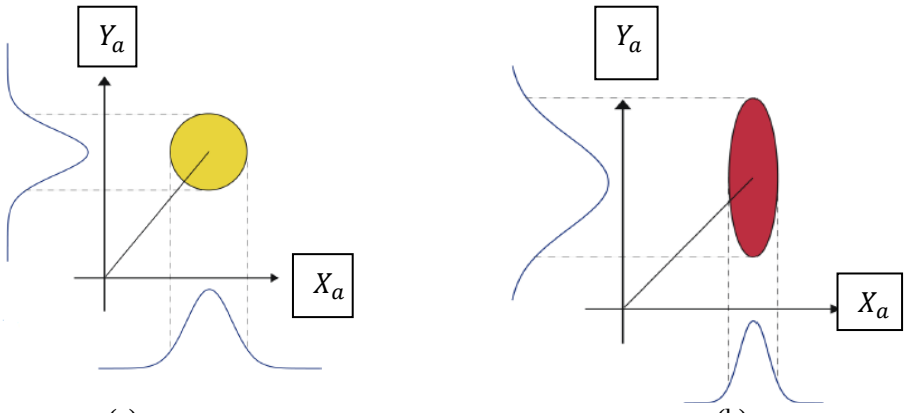

(a) (b)

Figure 2.3: Uncertainties of (a) coherent state (b) squeezed state

2.6.1.1 Types of squeezing

Different types of squeezed states are theoretically reported and experimentally observed for different optical and optomechanical systems with potential applications. These are quadrature squeezing, two mode squeezing, amplitude squared and cube squeezing, phase squeezing, difference and sum squeezing, n-th order single field mode squeezing and spin squeezing etc. We introduce the inequalities of different types of squeezing, in next subsection.

2.6.1.2 Inequalities of squeezing:

The two quadratures X_1 and X_2, express the real (electric) and the imaginary (magnetic) parts of an e. m. field, respectively. The quadrature operators follow the commutation relation $[X_1, X_2] = \frac{1}{2}C$, where C-number. Using the uncertainty relation the variance of the quadratures obey the following relation

$$\langle(\Delta X_1)^2\rangle\langle(\Delta X_2)^2\rangle \geq \frac{1}{16} |\langle C\rangle|^2 \tag{2.4}$$

where $\langle(\Delta X_i)^2\rangle = \langle X_i{}^2\rangle - \langle X_i\rangle^2$. The field quadrature is said to be squeezed if

$$\langle(\Delta X_i)^2\rangle - \frac{1}{4} |\langle C\rangle| \leq 0 \tag{2.5}$$

For single field mode, quadrature operators are $X_\sigma = \frac{\sigma(t)+\sigma^\dagger(t)}{2}$ and $Y_\sigma = \frac{\sigma(t)-\sigma^\dagger(t)}{2i}$. If the variance of the field quadratures obeys following condition, the quadrature is squeezed [97]

$$(\Delta X_\sigma)^2 < \frac{1}{4} \text{ and } (\Delta Y_\sigma)^2 < \frac{1}{4} \tag{2.6}$$

The operators for compound field modes (a, c) are

$$X_{ac} = \frac{a(t)+a^\dagger(t)+c(t)+c^\dagger(t)}{2\sqrt{2}} \ , \ Y_{ac} = \frac{a(t)-a^\dagger(t)+c(t)-c^\dagger(t)}{2\sqrt{2}i} \tag{2.7}$$

The condition for squeezing is

$$(\Delta X_{ac})^2 < \frac{1}{4} \ , \ (\Delta Y_{ac})^2 < \frac{1}{4} \tag{2.8}$$

For sum-squeezing the Y_i and C have the form [98]

$$Y_1 = \frac{1}{2}\{a(t)c(t) + a^\dagger(t)c^\dagger(t)\}, Y_2 = \frac{1}{2i}\{a(t)c(t) - a^\dagger(t)c^\dagger(t)\}, \ \ C = N_a + N_b + 1$$

The sum squeezing is possible in the Y_i direction if $S_{i_{ab}} < 0$ with $i = 1, 2$.

We define the squeezing factor as

$$S_{i_{ab}} = \langle(\Delta Y_i)^2\rangle - \frac{1}{4} \ | \langle C\rangle | \leq 0 \tag{2.9}$$

For difference squeezed states [64] the operators are

$$Z_1 = \frac{1}{2}\{a(t)b^\dagger(t) + a^\dagger(t)b(t)\}, \quad Z_2 = \frac{1}{2i}\{a(t)b^\dagger(t) - a^\dagger(t)b(t)\}, \ \ C = N_b - N_a$$

The difference squeezing is possible along the Z_i direction if $Q_{i_{ab}} < 0$ with $i = 1, 2$.

The squeezing factor are introduced here

$$Q_{i_{ab}} = \langle(\Delta Z_i)^2\rangle - \frac{1}{4} \ | \langle C\rangle | \leq 0 \tag{2.10}$$

For n-th order single field mode squeezing, operators are [99]

$$X_1 = \frac{1}{2}\{a^n(t) + a^{\dagger n}(t)\}, X_2 = \frac{1}{2i}\{a^n(t) - a^{\dagger n}(t)\}, \ \ C = a^n(t)a^{\dagger n}(t) - a^{\dagger n}(t)a^n(t)$$

The squeezing is possible in the X_i direction if $S_i(n) < 0$ where

$$S_i(n) = \langle(\Delta X_i)^2\rangle - \frac{1}{4} \ | \langle C\rangle | \leq 0 \tag{2.11}$$

Luks et al. criterion [100] of single mode principal squeezing is $\langle \Delta a^{\dagger} \Delta a \rangle < |\langle (\Delta a)^2 \rangle|$ and normal squeezing is $\langle \Delta a^{\dagger} \Delta a \rangle < Re\langle (\Delta a)^2 \rangle$ where $\Delta a = a - \langle a \rangle$.

We define the above two relations as follows:

$$P_s(a) = \langle \Delta a^{\dagger} \Delta a \rangle - |\langle (\Delta a)^2 \rangle| < 0 \tag{2.12}$$

$$N_s(a) = \langle \Delta a^{\dagger} \Delta a \rangle - Re\langle (\Delta a)^2 \rangle < 0 \tag{2.13}$$

Similarly, criteria for compound field mode [101, 102] are $\langle \Delta a_{12}^{\dagger} \Delta a_{12} \rangle < |\langle (\Delta a_{12})^2 \rangle|$ and $\langle \Delta a_{12}^{\dagger} \Delta a_{12} \rangle < Re\langle (\Delta a_{12})^2 \rangle$ respectively, where $a_{12} = a_1 + a_2$ and $\Delta a_{12} = a_{12} - \langle a_{12} \rangle$. The above two relations are defined as

$$P_s(ab) = \langle \Delta a_{12}^{\dagger} \Delta a_{12} \rangle - |\langle (\Delta a_{12})^2 \rangle| < 0 \tag{2.14}$$

$$N_s(ab) = \langle \Delta a_{12}^{\dagger} \Delta a_{12} \rangle - Re\langle (\Delta a_{12})^2 \rangle < 0 \tag{2.15}$$

Using ideas of second quantization and Schwinger-Bosonic representation [103], different spin operators are expressed in terms of two field modes $a^{\dagger}(b^{\dagger})$ and $a(b)$ are as follows: $S_x = \frac{1}{2}(S_+ + S_-)$, $S_y = \frac{1}{2i}(S_+ - S_-)$, $S_z = \frac{1}{2}(b^{\dagger}b - a^{\dagger}a)$ where $S_+ = b^{\dagger}a$ and $S_- = a^{\dagger}b$. The spin components satisfy the commutation relation $[S_i, S_j] = i\epsilon_{ijk}S_k$ where ϵ_{ijk} implies Levi-civita symbol. So, any pair of spin component follow the uncertainty relation $\langle (\Delta S_x)^2 \rangle \langle (\Delta S_y)^2 \rangle \geq \frac{1}{4}\langle S_z \rangle^2$ where $(\Delta S_x)^2 = \langle S_x^2 \rangle - \langle S_x \rangle^2$ is the variance along S_x direction. So, the conditions for spin squeezing along S_x and S_y are

$$\langle (\Delta S_x)^2 \rangle < \frac{1}{2}|\langle S_z \rangle| \, , \left\langle \left(\Delta S_y\right)^2 \right\rangle < \frac{1}{2}|\langle S_z \rangle| \tag{2.16}$$

We define the squeezing factors are as follows

$$S(x) = \frac{\langle (\Delta S_x)^2 \rangle}{\frac{1}{2}|\langle S_z \rangle|} < 1 \; ; \; S(y) = \frac{\left\langle \left(\Delta S_y\right)^2 \right\rangle}{\frac{1}{2}|\langle S_z \rangle|} < 1 \tag{2.17}$$

Using these criteria, we have investigated different types of squeezing, in chapter 3, 4 and 5.

2.6.2 Antibunching

Particle statistics are generally of three types. These are super-Poissonian, Poissonian and sub- Poissonian. First two statistics can be explained via classical wave theory. Last one, sub-Poissonian statistics has no classical explanation, corresponds to antibunching. Antibunching phenomenon is associated with the emission of single photon. For secured communication single photon source is one of the basic requirements [23, 104]. First experimental evidence [8] of single photon source was performed by HBT (H. Brown and R. Twiss) experiment. The experimental idea is based on intensity correlation (second-order correlation). The intensity correlation function is expressed by $g^2(\tau) = \frac{\langle I(t)I(t+\tau)\rangle}{\langle I(t)\rangle\langle I(t+\tau)\rangle}$. For different cases the values of the correlation function with zero time delay $g^2(0)$ are as follows: for antibunched light $g^2(0) < 0$, random or coherent $g^2(0) = 0$ and bunched or chaotic light $g^2(0) > 0$. Figure 2.4 depicts the variation of the spacing of photon for three distinct cases. In next subsection, we have discussed the inequalities of lower order as well as higher order antibunching.

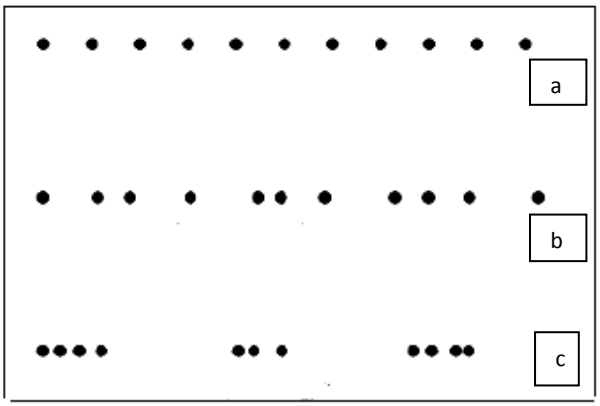

Figure 2.4: Photon stream comparison of (a) antibunching (b) coherent (c) bunched light.

2.6.2.1 Inequalities of Antibunching

Lower order particle statistics is quantified via Mandel's Q parameter [105, 106] and it is defined as

$$Q = \frac{V_n}{<n>} - 1 \tag{2.18}$$

where n implies particle number $n = a^\dagger a$ and $V_n =< n^2 > -< n >^2$. The factor $Q < 0, Q = 0$ and $Q > 0$ are related to sub-Poissonian (antibunching), Poissonian (coherent) and super- Poissonian (bunching) statistics, respectively. So, from expression (2.18), the criteria for single field mode is defined as $A_a < 0$ where

$$A_a =< a^{\dagger 2} a^2 > -< a^\dagger a >^2 \tag{2.19}$$

Similarly, for compound field mode the parameter $A_{ab} < 0$ with

$$A_{ab} =< a^\dagger b^\dagger b a > -< a^\dagger a >< b^\dagger b > \tag{2.20}$$

Lee criteria [107], for higher-order antibunching is expressed via factorial moment of the number operator, the inequality is given by

$$\langle N_a^{l+1}\rangle\langle N_a^{m-1}\rangle < \langle N_a^l\rangle\langle N_a^m\rangle \tag{2.21}$$

where N_a is the number operator for a mode, l-th order factorial moment of it is given by $\langle N_a^l\rangle = \prod_{i=0}^{l-1}(N_a - i)$, l, m are integers ($l \geq m \geq 1$). For m = 1 the above criterion is reduced to $\langle N_a^{l+1}\rangle < \langle N_a\rangle^l\langle N_a\rangle$. The condition for l-th order antibunching is

$$A_a(l) = \langle N_a^{l+1}\rangle < \langle N_a\rangle^{l+1} < 0 \tag{2.22}$$

$\langle N_a^l\rangle = \langle a^{\dagger l} a^l\rangle$ measures l photons of the mode at a fixed point in space-time coordinate. The inequality indicates the probability of the detection of a single photon pulse is greater than from two photons in a bunch and so on. This typical feature is important for quantum cryptography. For l = 1, the condition corresponds to lower

order while $l \geq 2$ is implies higher-order. Again, for compound mode *ab* the criterion is expressed by the following inequality [107]

$$\langle N_a^{l+1} N_b^{m-1} + N_b^{l+1} N_a^{m-1} \rangle < \langle N_a^l N_b^m + N_b^l N_a^m \rangle \tag{2.23}$$

with $l \geq m \geq 1$. For $m = 1$ the above condition becomes

$$\langle N_a^{l+1} + N_b^{l+1} \rangle < \langle N_a^l N_b + N_b^l N_a \rangle$$

We define, the antibunching factor for l-th order compound field mode as

$$A_{ab}(l) = \langle N_a^{l+1} + N_b^{l+1} \rangle - \langle N_a^l N_b + N_b^l N_a \rangle < 0 \tag{2.24}$$

2.6.3 Entanglement, EPR Steering and Bell states

Quantum entanglement is one of the fundamental aspects in the field of quantum optics. In quantum computation entangled state plays the key role. Entangled state means non-separable state and essentially non-classical. When multi particles are connected together or interact physically in such a manner that wave function of the system can't factorized into the product of individual particle wave function. If $|\psi\rangle$ denotes the total system wave function then it follows $|\psi\rangle \neq |\psi_1\rangle \otimes |\psi_2\rangle \otimes |\psi_3\rangle \ldots$. Similarly, in case of mixed state the density matrix has the form $\rho \neq \sum_i p_i \rho_1^i \otimes \rho_2^i \otimes \ldots$. This has potential advantages in QIP via dense coding, teleportation, quantum cryptography [26, 108, 109]. Another two multi particle correlations are steerable state and Bell state. Einstein, Podolosky, and Rosen (1935) made a question about completeness of quantum formalism [5]. To realize the quantum formalism many efforts have been taken via different types of quantum nonlocality. Such nonlocalities are Bell nonlocality, EPR steering and entanglement. The idea of EPR steering was explained by Schrodinger in 1935 as a generalisation of EPR-paradox [110]. It explains remote manipulation of quantum state. Bell states are maximally entangled state. Wener established that all

entangled or non-separable states are not Bell non-local [111]. The relationship between three correlations was introduced by H. Wiseman et al [112, 113]. Entangled state is superset of EPR Steerable state and Bell state is subset of steerable state (figure 2.5). In next section, we introduce different inseparability criteria and using these criteria the possibilities of nonclassicalities are discussed chapter 3, 4 and 5.

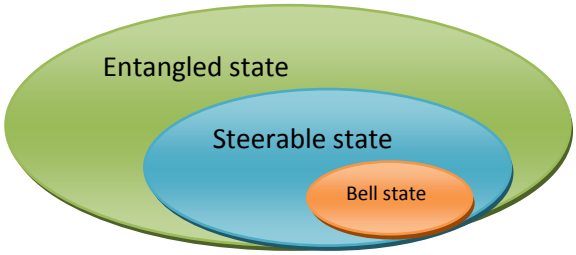

Figure 2.5: Representations of entangled, steerable and Bell state

2.6.3.1 The inequalities of two mode quantum entanglement

There are a number of inseparability criteria to characterize entangled states, which are sufficient but not necessary. First, to find the existence of entanglement for two field mode state, we use Duan *et al* [114] formula which is derived an inequality interms of the linear combination of position and momentum. This can be expressed in terms of moments of raising (lowering) operators between two field modes as $(\Delta u)^2 + (\Delta v)^2 < 2$.

$$u = \frac{a(t)+a^{\dagger}(t)+c(t)+c^{\dagger}(t)}{\sqrt{2}} \quad \text{and } v = \frac{a(t)-a^{\dagger}(t)+c(t)-c^{\dagger}(t)}{\sqrt{2}i} \tag{2.25}$$

The condition defined as $e_{ac} < 0$

$$e_{ac} = (\Delta u)^2 + (\Delta v)^2 - 2 \tag{2.26}$$

Second, Hillery-Zubairy inseparability criteria [115, 116] are expressed via moments of the field operators. For seperable state the criteria for two field modes (a, c) are $\left|\langle ac^{\dagger}\rangle\right|^2 > \langle N_a N_c\rangle$ and $|\langle ac\rangle|^2 > [\langle N_a\rangle\langle N_c\rangle]$ where N_a , N_c are the number operators corresponds to the field modes.

So, the conditions for two mode entanglement in lower order are defined as $E_{ac} < 0$ and $E'_{ac} < 0$. These two named as Hillery-Zubairy criterion 1 and Hillery-Zubairy criterion 2, respectively.

$$E_{ac} = \begin{vmatrix} \langle N_a N_c\rangle & \langle a^{\dagger} c\rangle \\ \langle ac^{\dagger}\rangle & 1 \end{vmatrix} \tag{2.27}$$

$$E'_{ac} = \begin{vmatrix} \langle N_a\rangle & \langle a^{\dagger} c^{\dagger}\rangle \\ \langle ac\rangle & \langle N_c\rangle \end{vmatrix} \tag{2.28}$$

Higher order study has also importance, in which degree of nonclassicality is expected to be enhanced. The criteria for higher order studies are as follows: Hillery-Zubairy criteria [115, 116] are one which is sufficient to characterize higher-order entanglement. Starting from the expressions of the quadratic operators $L_1 = \{a^m c^{\dagger n} + a^{\dagger m} c^n\}$ and $L_2 = -i\{a^m c^{\dagger n} - a^{\dagger m} c^n\}$ and applying uncertainty relation and Schwarz inequality Hillery and Zubairy formulated that the states to be non-separable if $|\langle a^m c^{\dagger n}\rangle| > [\langle a^{\dagger m} a^m c^{\dagger n} c^n\rangle]^{\frac{1}{2}}$. Similarly for the operators $F_1 = \{a^m c^n + a^{\dagger m} c^{\dagger n}\}$ and $F_2 = -i\{a^m c^n - a^{\dagger m} c^{\dagger n}\}$ they established that the product state would be non-separable if $|\langle a^m c^n\rangle| > [\langle a^{\dagger m} a^m\rangle\langle c^{\dagger n} c^n\rangle]^{\frac{1}{2}}$ where m and n are non-zero positive integers. For product state choice of the integers m, n satisfy the condition $m + n \geq 3$.

$$E_{ac}(m,n) = \begin{vmatrix} \langle a^{\dagger m} a^m c^{\dagger n} c^n \rangle & \langle a^{\dagger m} c^n \rangle \\ \langle a^m c^{\dagger n} \rangle & 1 \end{vmatrix} \tag{2.30}$$

$$E'_{ac}(m,n) = \begin{vmatrix} \langle a^{\dagger m} a^m \rangle & \langle a^{\dagger m} c^{\dagger n} \rangle \\ \langle a^m c^n \rangle & \langle c^{\dagger n} c^n \rangle \end{vmatrix} \tag{2.31}$$

Agarwal and Biswas established two inequalities [117] regarding two-mode separable states by introducing higher-order correlation between the momentum and position coordinates. First, using a group of operators (angular momentum operators) $S_x = \frac{1}{2}(a^\dagger c + a c^\dagger)$, $S_y = \frac{1}{2i}(a^\dagger c + a c^\dagger)$, $S_z = \frac{1}{2}(a^\dagger a - c^\dagger c)$ and uncertainty relation $\Delta S_x \Delta S_y \geq \frac{1}{2}|\langle S_z \rangle|$ and also taking partial transpose, they established following relation for separable states $[\langle a^\dagger a c c^\dagger \rangle + \langle a a^\dagger c^\dagger c \rangle + \langle a^{\dagger 2} c^{\dagger 2} \rangle + \langle a^2 c^2 \rangle - \langle a^\dagger c^\dagger + a c \rangle^2] \times [\langle a^\dagger a c c^\dagger \rangle + \langle a a^\dagger c^\dagger c \rangle - \langle a^{\dagger 2} c^{\dagger 2} \rangle - \langle a^2 c^2 \rangle + \langle a^\dagger c^\dagger - a c \rangle^2] \geq \left|\langle a^\dagger a - c^\dagger c \rangle\right|^2$

For two mode non-separable state the condition is $G_{ac} < 0$.

where $G_{ac} = [\langle a^\dagger a c c^\dagger \rangle + \langle a a^\dagger c^\dagger c \rangle + \langle a^{\dagger 2} c^{\dagger 2} \rangle + \langle a^2 c^2 \rangle - \langle a^\dagger c^\dagger + a c \rangle^2] \times [\langle a^\dagger a c c^\dagger \rangle + \langle a a^\dagger c^\dagger c \rangle - \langle a^{\dagger 2} c^{\dagger 2} \rangle - \langle a^2 c^2 \rangle + \langle a^\dagger c^\dagger - a c \rangle^2] - \left|\langle a^\dagger a - c^\dagger c \rangle\right|^2$ (2.32)

Second, using a group of operators $K_x = \frac{1}{2}(a^\dagger c^\dagger + a c)$, $K_y = \frac{1}{2i}(a^\dagger c^\dagger - a c)$, $K_z = \frac{1}{2}(a^\dagger a + c^\dagger c + 1)$ satisfying $SU(1,1)$ algebra and uncertainty relation they established the following inequality for separable states

$$[\langle a^\dagger a c^\dagger c \rangle + \langle a a^\dagger c c^\dagger \rangle + \langle a^{\dagger 2} c^2 \rangle + \langle a^2 c^{\dagger 2} \rangle - \langle a^\dagger c + a c^\dagger \rangle^2] \times [\langle a^\dagger a c^\dagger c \rangle + \langle a a^\dagger c c^\dagger \rangle - \langle a^{\dagger 2} c^2 \rangle - \langle a^2 c^{\dagger 2} \rangle + \langle a^\dagger c - a c^\dagger \rangle^2] \geq \left|\langle a^\dagger a + c^\dagger c \rangle\right|^2$$

For two mode non-separable state the condition is $A_{ac} < 0$.

Where $A_{ac} = [\langle a^\dagger a c^\dagger c\rangle + \langle a a^\dagger c c^\dagger\rangle + \langle a^{\dagger 2} c^2\rangle + \langle a^2 c^{\dagger 2}\rangle - \langle a^\dagger c + a c^\dagger\rangle^2] \times$

$[\langle a^\dagger a c^\dagger c\rangle + \langle a a^\dagger c c^\dagger\rangle - \langle a^{\dagger 2} c^2\rangle - \langle a^2 c^{\dagger 2}\rangle + \langle a^\dagger c - a c^\dagger\rangle^2] - \left|\langle a^\dagger a + c^\dagger c\rangle\right|^2$ (2.33)

2.6.3.2 The Inequalities of three and four mode entanglement

To examine the possibilities of three and four field mode entanglement, we have used Li et al moment based criteria [118]. Using group of operators $L_1 = abc^\dagger + a^\dagger b^\dagger c$ and $L_2 = i(abc^\dagger - a^\dagger b^\dagger c)$ and Schwarz inequality, Li et al formulated the condition $\langle N_a N_b N_c\rangle \geq \left|\langle abc^\dagger\rangle\right|^2$ for tri-modal entanglement. Again, for the set of operators $K_1 = ab^\dagger c + a^\dagger b c^\dagger$ and $K_2 = i(ab^\dagger c - a^\dagger b c^\dagger)$ and Schwarz inequality, Li et al formulated another condition $\langle N_a\rangle\langle N_b\rangle\langle N_c\rangle \geq |\langle abc\rangle|^2$. The violations of above inequalities imply the signature of tri-modal entanglement. We recall the two relations as

$$\zeta = \langle N_a N_b N_c\rangle - \left|\langle abc^\dagger\rangle\right|^2 \quad (2.34)$$

$$\varepsilon = \langle N_a\rangle\langle N_b\rangle\langle N_c\rangle - |\langle abc\rangle|^2 \quad (2.35)$$

$\zeta < 0$ and $\varepsilon < 0$ give the signature of entanglement. We rename equation (2.34) and (2.35) as Li et al criterion 1 and 2.

Again, Li et al formulated the inequality for four field modes [118], which is given by $\langle N_a\rangle\langle N_b\rangle\langle N_c\rangle\langle N_d\rangle \geq |\langle abcd\rangle|^2$. The violation of the inequality implies the possibility of four field mode entanglement. We define this as

$$E = \langle N_a\rangle\langle N_b\rangle\langle N_c\rangle\langle N_d\rangle - |\langle abcd\rangle|^2 \quad (2.36)$$

Four-mode entangled state exists if $E < 0$. We have analyzed three and four field mode entanglement in chapter 4, using above inequalities.

2.6.3.3 Inequalities of EPR steering and Bell states

There are several inequalities for EPR steering: Reid criteria using uncertainty principle [119], Walborn criteria using an entropic formulation [120], Cavalcanti *et al* criteria using moment based inequalities [121]. Violations of steering inequalities investigated theoretically and obseved experimentally, recently [122-127]. The Cavalcanti *et al* criteria for two modes EPR-steerable state is

$$\left|\langle a_i a_j{}^{\dagger}\rangle\right|^2 \leq \langle a_i^{\dagger} a_i (a_j^{\dagger} a_j + \tfrac{1}{2})\rangle$$

The violation of the inequality signifies the possibility of EPR-steering. For two remote observer, Alice and Bob, share a pair of nonseparable particle if Alice measures mode a_i and Bob measures mode a_j then violation of the inequality signifies that Bob would be able to steer Alice or vice versa. Using this inequality we define a correlation function ξ_{ij} which gives the signature of EPR-steering when $\xi_{ij} > 0$.

$$\xi_{ij} = \left|\langle a_i a_j{}^{\dagger}\rangle\right|^2 - \langle a_i^{\dagger} a_i \left(a_j^{\dagger} a_j + \tfrac{1}{2}\right)\rangle \tag{2.37}$$

Similarly, for Bell states [6, 7] the codition is $\zeta_{ij} > 0$, where

$$\zeta_{ij} = \left|\langle a_i a_j{}^{\dagger}\rangle\right|^2 - \langle\left(a_i^{\dagger} a_i + \tfrac{1}{2}\right)\left(a_j^{\dagger} a_j + \tfrac{1}{2}\right)\rangle \tag{2.38}$$

In chapter 5, we have analyzed above two correlations in PT-symmetric micro-cavity system and stated possible utility.